"Enhanced Wellbore Stabilization and Reservoir Productivity with Aphron Drilling Fluid Technology"

QUARTERLY PROGRESS REPORT

July 1 – September 30, 2004

by

Fred Growcock

Issued October, 2004

DOE Award Number DE-FC26-03NT42000

MASI Technologies *LLC*
5950 N. Course Dr.
Houston, Texas 77072

DISCLAIMER

ABSTRACT

During this fourth Quarter of the Project, all of the remaining tasks of Phase I were completed. These included (a) In Situ Visualization, (b) Aphron Air Diffusivity, (c) Aphron Shell Hydrophobicity, and (d) Sealing of Permeable and Fractured Media.

Among the highlights of the work conducted during this Quarter was the finding that aphrons can survive compression to at least 4000 psi. Initial reaction of aphrons to an increase in pressure is similar to that of conventional bubbles in that the aphron shrinks in size as predicted by the modified Ideal Gas Law. However, conventional bubbles lose air rapidly at elevated pressures, and they continue to shrink at a high rate, disappearing within seconds. Aphrons shrink much more slowly. The rate of shrinkage depends on fluid composition, bubble size, and rate of pressurization and depressurization. Another, but less important, factor is loss of oxygen via chemical reaction with some components in the mud, a process that can take a few minutes to a few hours (depending on temperature and pressure), which results in aphrons that are filled mainly with nitrogen.

This continuous shrinkage of aphrons at elevated pressure is caused primarily by slow diffusion of air from the aphrons and dissolution of the expelled air in the aqueous medium. When the aphrons reach a critical minimum size, they undergo a structural change that leads to their rapid demise. However, depressurization of the fluid to a sufficiently low pressure results in supersaturation of the aqueous medium, and the air is released in a process that can take minutes; the released air preferentially enters existing aphrons, though new aphrons can also be formed.

Although the amount of air in a typical aphron drilling fluid is very small (15% v/v air at ambient conditions constitutes only 0.02% w/w), aphrons can affect the invasion rate of the fluid due to the phenomenon of bubbly flow. Flow visualization experiments demonstrate that, under the influence of a pressure differential, aphrons move at a velocity much greater than the liquid phase. Thus, they can accumulate at the fluid front and inhibit movement of the liquid. Other tests indicate that aphrons have little affinity for each other or for the mineral surfaces in the rock; thus, they resist agglomeration and coalescence and can be pushed back out of the rock easily by reversing the pressure differential.

TABLE OF CONTENTS

LIST OF FIGURES

INTRODUCTION

Aphron drilling fluids have been successfully used in 300+ applications worldwide to drill depleted reservoirs in mature oil and gas fields, high-permeability formations and microfractured rock. These fluids serve as a successful and cost-effective alternative to underbalanced drilling for avoidance of whole fluid loss and differential sticking.[1-4]

There are two chief attributes of these fluids that permit a decrease of fluid invasion and damage to the formation. First, the properties of the base fluid are such that upon entering a loss zone, the flow rate is speculated to decrease dramatically. This is thought to occur because the bulk fluid is very highly shear-thinning and possesses a very high LSRV (Low-Shear-Rate Viscosity). Second, very tough and flexible microbubbles are incorporated into the bulk fluid with conventional mud mixing equipment. These highly stabilized bubbles, or "aphrons," are essential to sealing the problem area by forming an internal bridge that acts as a loss circulation material.

Water-based aphrons, as found in APHRON ICS™ and HYSSTER™ systems, are the subject of this study. They consist of two essential elements: a spherical core of air and a protective outer shell.[5] In contrast to a conventional air bubble, which is stabilized by a surfactant monolayer, the outer shell of the aphron is thought to consist of a much more robust surfactant tri-layer. This tri-layer is envisioned as consisting of an inner surfactant film enveloped by a viscous water layer, outside of which an outer bilayer of surfactants provides rigidity and low permeability to the structure while imparting some hydrophilic character to it. Under quiescent conditions, the structure is compatible with the aqueous bulk fluid, but when enough shear or compression is applied to the aphron, e.g. when bridging a pore network, the outermost shell layer is stripped, rendering the aphron hydrophobic.[5]

Aphrons are claimed to act as a unique bridging material, forming a micro-environment in a pore network or fracture that appears to behave in some ways like a foam, and in other ways like a solid, but flexible bridging material. As is the case with any bridging material, concentration and size of the aphrons are critical to the mud's ability to seal thief zones. Aphrons are created and entrained in the bulk fluid with standard mud mixing equipment, which reduces the safety con-

cerns and costs associated with high-pressure hoses and compressors commonly utilized in air or foam drilling.[6] Although each application is customized for the individual operator's needs, the mud system is generally designed to contain 12-15% by volume air. Aphrons are thought to be sized or polished at the drill bit to achieve a size of 15-100 μm diameter, which is typical of many bridging materials.

Many aspects of the aphron and its physicochemical properties should be evaluated further to determine ways to enhance aphron performance. Greater application of this novel technology and the consequent reduction in drilling costs would be facilitated greatly by a systematic and thorough evaluation of the structure and behavior of aphron drilling fluids downhole.

The objectives of this project are threefold: (a) develop a comprehensive understanding of how aphrons behave at elevated pressures and temperatures; (b) measure the ability of aphron drilling fluids to seal permeable and fractured formations under simulated downhole conditions; and (c) determine the role played by each component of the drilling fluid.

The Project is divided into two phases. Phase I (Year 1) is focused on developing evidence for the ways in which aphrons behave differently from ordinary surfactant-stabilized bubbles, particularly how they seal permeable and micro-fractured formations during drilling operations. Various methods are evaluated for characterizing the properties of aphrons, including acoustic bubble spectroscopy, optical and electronic micro-imaging and interfacial tension. Key properties to be investigated include the effects of pressure on bubble size, the influence of environmental parameters on aphron stability, the affinity of aphrons for each other and for the mineral surfaces in rock pores and microfractures, and the nature of aphron seals in fractures and pore networks. Initial sealing and formation damage tests also will be carried out, using lab-scale apparati designed to simulate permeable and micro-fractured environments. Phase II (Year 2) focuses on optimization of the structure of aphrons and composition of aphron drilling fluids, quantifying the flow properties of the fluids (radial vs linear flow, shear and extensional viscosity effects and bubbly flow phenomena), and understanding formation sealing and damage under simulated downhole conditions (including scale-up tests), so as to furnish irrefutable evidence for the this technology and provide field-usable data.

The current schedule of tasks is provided in Figure 1.

Figure 1. Schedule of Tasks in Aphron Drilling Fluid Project

	2003	2004				2005		
Task	4th Q	1st Q	2nd Q	3rd Q	4th Q	1st Q	2nd Q	3rd Q
1. Aphron Compressibility								
1.1 Aphron Visualization	X	X	X					
1.2 Fluid Density	X	X	X					
1.3 Aphron Air Diffusivity	X	X	X	X				
2. Sealing Mechanism								
2.1 In Situ Visualization			X	X				
2.2 Pressure Transmissibility	X	X	X					
2.3 Aphron Shell Hydrophobicity			X	X				
3. Leak-Off/Formation Damage - Initial Tests								
3.1 Sealing of Permeable Media			X	X				
3.2 Sealing of Fractured Media			X	X				
4. Aphron Optimization								
4.1 Microstructure								
4.2 Performance								
5. Flow Properties								
5.1 Geometry of Medium								
5.2 Fluid Rheology								
5.3 Multi-Phase Flow Effects								
6. Leak-Off/Formation Damage Perm Media								
6.1 Lab Tests Leak-Off/Return Perm								
6.2 Field-Sim Tests Leak-Off/Return Perm								

Phase I runs from Oct. 1, 2003 through Sept. 30, 2004 and consists of Task Areas 1-3. All of these have been completed, as scheduled, and are indicated by an X.

EXECUTIVE SUMMARY

All eight tasks undertaken in this first year of the project (Phase I) were completed by the conclusion of Phase I. All of these tasks focused on the properties of aphrons. Four tasks were completed in the 4th Quarter (3rd Q 2004): (a) *In Situ* Visualization – evaluation of acoustic and optical methods for measuring bubble size distribution (BSD) in a pressurized and heated environment; (b) Aphron Air Diffusivity – determination of the effects of pressure, rate of compression and chemical composition on aphron stability; (c) Aphron Shell Hydrophobicity – determination of the affinity of aphrons for each other and the walls of pores and microfractures in reservoir rock; and (d) Sealing of Permeable and Fractured Media – measurement of the effects of pressure, temperature and nature of permeable rocks on the invasion profile of aphron drilling fluids.

For the *In situ* Visualization task, a high-pressure high-temperature circulating system (20.7 MPa, or 3000 psi, and 121 ^{o}C, or 250 ^{o}F) was completed and modified with a viewing port to enable simultaneous Acoustic Bubble Spectroscopy (ABS) and optical imaging. Tests carried out in high-viscosity fluids like the APHRON ICS^{TM} system at a pressure of 2000 psi, with and without flow, gave a similar result to that observed in earlier ambient pressure tests, namely that bubble size distribution (BSD) measured via ABS does not correlate well with BSD determined via optical imaging. The main problem appears to be that the algorithm used in the ABS does not treat high viscosity or shear-thinning fluids properly, resulting in insensitivity to large bubbles and skewing of the BSD to very low values. In addition, the method does not provide any data for bubbles smaller than 10 µm diameter, though this is a minor limitation. Direct optical imaging, on the other hand, not only reveals the dimensions of a population of bubbles, but also the dimensions of single bubbles, so that the technique can be used to characterize the effects of environmental variables on bubble size. The development of an ultra-thin high-pressure viewing cell enables imaging of opaque fluids, too, thus obviating the need for the ABS. This viewing cell was used to carry out the Aphron Air Diffusivity task.

In the course of fulfilling the deliverables of the Air Diffusivity task, it was found that aphrons can survive compression to at least 4000 psi. The number of visible aphrons at that pressure is small, and the survivors have a limited life. Nevertheless, this finding is of enormous significance, in that it provides the first clear evidence that aphron technology may be useful at higher pressures (3000 psi) than previously thought. Compression of large aphrons initially results in volume reduction that is inversely proportional to the absolute pressure, as is the case for conventional bubbles. However, the latter do not survive a few hundred psi for more than a few seconds, whereas aphrons can survive a few thousand psi for at least a few minutes. After initial compression to a fixed pressure, bubbles (including aphrons) continue to shrink at a rate that depends on a number of factors, including fluid composition, bubble size, and rate of pressurization. Another, but less important, factor is loss of oxygen via chemical reaction of the oxygen with some components in the mud, resulting in aphrons that are filled mainly with nitrogen. Continuous shrinkage of bubbles at elevated pressure is caused primarily by diffusion of air out of the bubble and dissolution of the expelled air in the aqueous medium. For aphrons, the rate of diffusion of air is orders of magnitude lower than for conventional bubbles. However, when the

aphrons reach a critical minimum size, on the order of 50 µm diameter, they undergo a structural change that leads to fairly rapid collapse, and the aphrons disappear.

When an aphron system at elevated pressure is depressurized, surviving aphrons increase in size as per the modified Ideal Gas Law. Air that was lost from aphrons at elevated pressure and is in solution can be released if the pressure is reduced to a level low enough that the aqueous medium becomes supersaturated with air. The released air preferentially enters existing aphrons, but new aphrons can be formed, too.

Other tests indicate that aphrons have very little affinity for each other or for the mineral surfaces in rock formations encountered during drilling. Thus, aphrons resist agglomeration and coalescence and can be pushed back out easily by reversing the pressure differential, thus minimizing formation damage.

The role played by aphrons in controlling invasion of the drilling fluid in permeable media was elucidated. Leak-Off tests were carried out with a triaxial loading core leak-off tester capable of pressures up to 17 MPa (2500 psi) and temperatures up to 177 ^{o}C (350 ^{o}F). These tests demonstrated that the base fluid is primarily responsible for sealing permeable zones, and is capable of sealing rock as permeable as 80 darcies. However, properly designed aphrons can reduce these losses even further. It was learned that, although the amount of air in a typical aphron drilling fluid is very small (15% v/v air at ambient temperature and pressure constitutes only 0.02% w/w), aphrons can affect the invasion rate of the fluid because of the phenomenon of bubbly flow. Flow visualization experiments demonstrate that, under the influence of a pressure differential, aphrons move at a velocity much greater than the liquid phase. Thus, they can accumulate at the fluid front and inhibit movement of the liquid.

Several opportunities presented themselves to share the latest aphron drilling fluid technology with potential clients. These included the following:

- 3rd Quarter DEA Meeting in Houston Aug. 19.
- Operations Meeting of Shell Exploration & Production Co. (SEPCO) in New Orleans, Aug. 26.
- Meeting with faculty and students at Texas A&M University (College Station, TX) on Sept. 9 to discuss the possibility of collaborating on the mechanics of bubbly flow, a task scheduled to be addressed in Phase II.
- SPE Annual Technology Conference and Exhibition Sept 27-29.

Other events worthy of note included training of three team members at the M-I SWACO Customer Mud School, training by three other members in the use of LabView, and the consolidation and move of MASI Technology LLC to a new location: 8275 El Rio, Suite 130, Houston, TX 77054.

EXPERIMENTAL APPROACH

The methodologies used for the current tasks are detailed below:

In Situ Visualization

The HTHP Circulating System was completed this Quarter, and is shown in Figure 2. It is designed to safely sustain a target pressure of 20.7 MPa (3000 psia) and temperature of 121 ^{o}C (250 ^{o}F). While commissioning tests of the HTHP Circulating System have begun, a by-pass containing the Viewing Cell shown in Figure 3 was added so that both ABS and optical imaging could be carried out at the same time.

Figure 2. HTHP Circulating System

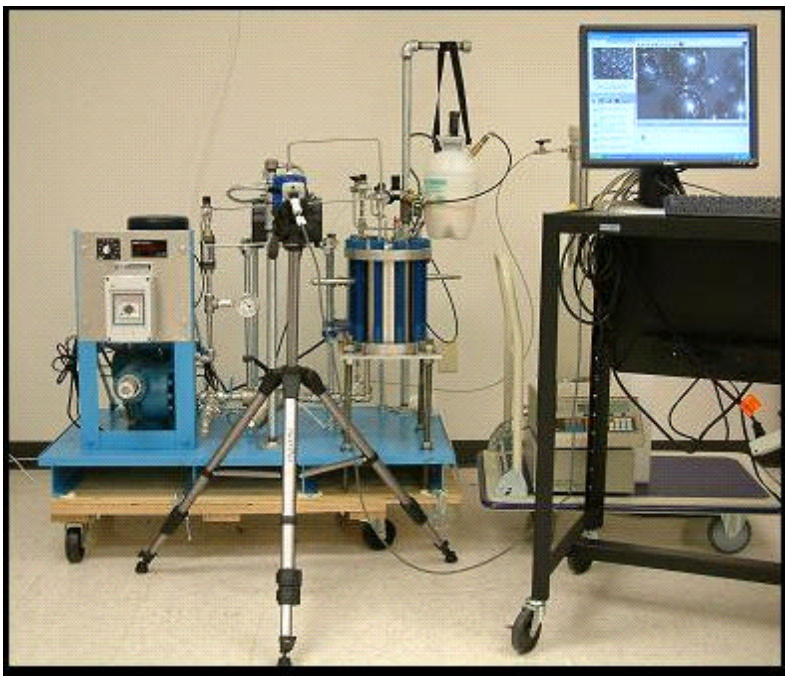

Figure 3. Close-Up View of HTHP Circulating System & Viewing Cell

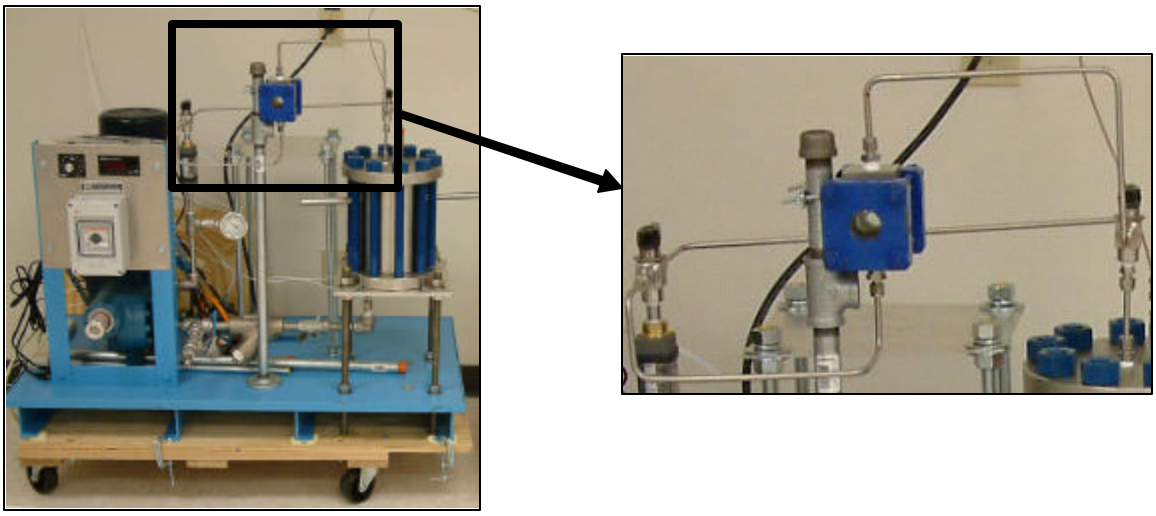

The Circulating System requires a fluid volume of about 1 ½ gal and, for validation, a transparent fluid system. The fluid that was developed for this purpose, dubbed the Transparent APHRON ICS™ drilling fluid, is similar in composition to the APHRON ICS™ system, but does not contain any of the opaque components. This fluid system possesses key properties, such as rheology and bubble stability, that are similar to the APHRON ICS™ system.

Aphron Air Diffusivity

The original method that was devised to measure the diffusion rate of air from aphrons involved monitoring the concentration of dissolved oxygen (DO) in the environment around the aphrons. However, it was found that, not only are the DO probes not suitable for high temperatures and pressures, DO itself changes very rapidly independent of diffusion. Indeed, it was found that DO depletes very rapidly (within just a few hours at ambient temperature and pressure) as a result of chemical reaction with some of the components in APHRON ICS™ drilling fluids. Consequently, a different method was devised for measuring air diffusivity. This technique relies on optical imaging of individual aphrons to monitor the bubble size as a function of time. However, the glass sight flow cell shown in Figure 3 was found to be unsuitable for looking at whole drilling fluids, inasmuch as the depth of the opaque fluids is too great to admit sufficient light for proper viewing.

Figure 4. Variable-Reservoir-Depth Polycarbonate Viewing Cell

Front View of Cell

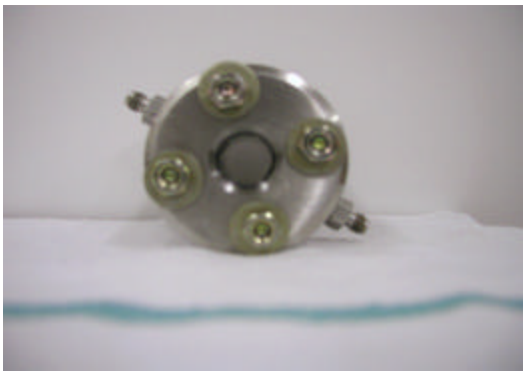

Side View of Cell

Disassembled Cell

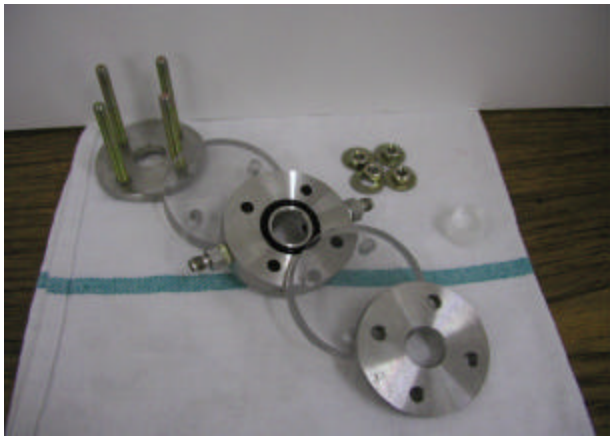

Although the lighting problem is minimized by using the transparent version of the APHRON ICS™ fluid, uncertainty in the depth of the bubbles creates a large uncertainty in bubble size determination. Furthermore, some tests need to be carried out with the standard (opaque) mud. Consequently, a new viewing cell was designed and constructed to provide a variable fluid reservoir depth (as shallow as 1 mm). This new sample cell, made of steel with ½" polycarbonate windows, promises to be useful for microscopic work to pressures of 4,000 psi. Photos of the cell are shown in Figure 4.

Most of the tests in the Variable-Reservoir-Depth Viewing Cell were conducted either with the Transparent Enhanced APHRON ICS™ fluid or with one of the regular APHRON ICS™ systems:

Table 1. Formulations of Whole APHRON ICS™ Drilling Fluids

		Quantity per Lab Equivalent Barrel		
Component	**Unit**	**Standard**	**Enhanced**	**SuperEnhanced**
Water	mL	338	337	337
Soda Ash	g	3	3	3
X-CIDE	mL	0.1	0.1	0.1
GO-DEVIL II	g	5	5	5
ACTIVATOR I	g	5	5	5
ACTIVATOR II	g	2	2	2
BLUE STREAK	mL	0.91	0.91	0.91
EMI-779	mL		0.5	0.5
EMI-780	g		0.5	0.5
EMI-802	mL			0.3

A microscope camera was obtained along with Vision Assistant, some optical imaging software from National Instruments, to monitor the effects of environmental variables on bubble size distribution and track individual bubbles. The software consists of image functions that extract and alter the structure of objects in an image using transformations to delineate objects and prepare them for quantitative inspection analysis.

A photomicrographic image of a Transparent APHRON ICS™ sample analyzed through Vision Assistant is shown in Figure 5. Filling of the bubbles, followed by compiling the data on surface area or diameter of the filled circles, will generate a bubble size distribution.

Figure 5. Example of Output Screen from Vision Assistant Software

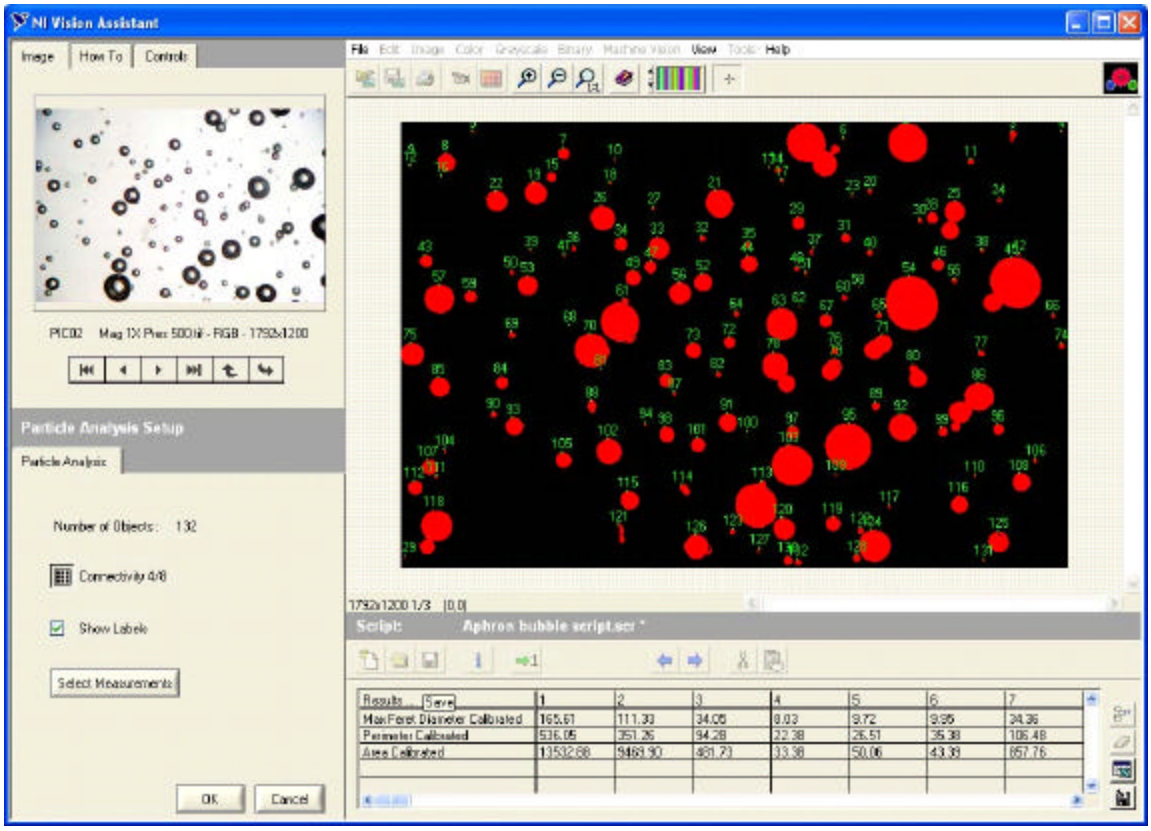

Aphron Shell Hydrophobicity

Several test methods were tried to measure the stickiness of bubbles. A schematic of one of the first devices is shown in Figure 6. A transparent APHRON ICS™ mud sample is placed in the chamber of a syringe. The aphrons are filtered and compressed while driving the bulk fluid through a fine glass filter that prevents passage of the aphrons. The syringe is then back-filled with the same aphron-free fluid to its initial volume and the number of bubbles that have agglomerated, coalesced and/or stuck to the walls of the chamber are counted.

Figure 6. Aphron Hydrophobicity Apparatus

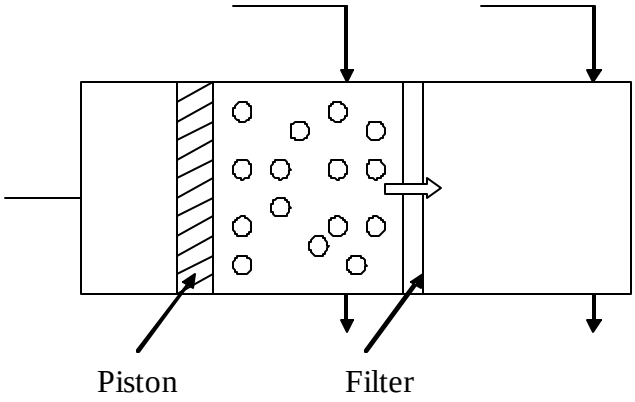

A modification of the apparatus shown in Figure 6 employs two glass syringes connected with a disposable filter of pore size much smaller than the average bubble size. A photograph of this apparatus fitted with a syringe pump is shown in Figure 7.

Figure 7. Dual Syringe Hydrophobicity Apparatus Fitted with Syringe Pump

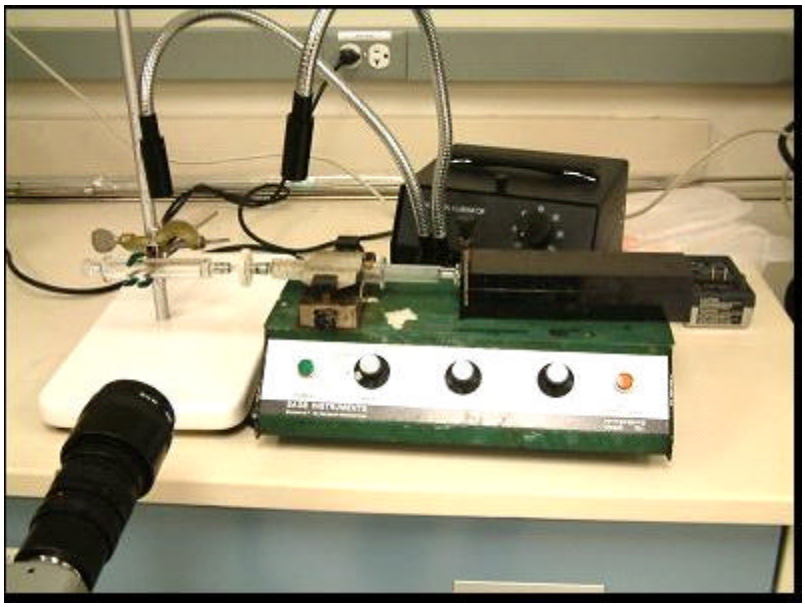

Other techniques were also tried, and these are discussed in the Results section.

Sealing of Permeable and Fractured Media

These two tasks utilize the same approach but with different types of porous media. A Core Leak-Off Test Apparatus was constructed from a Temco coreholder. The device enables radial and axial loading of cores up to 6 inches in length, pressures up to 17.3 MPa (2500 psi) and temperatures up to 177 ^{o}C (350 ^{o}F). A schematic of this apparatus is shown in Figure 8:

Figure 8. Schematic of Leak-Off Tester

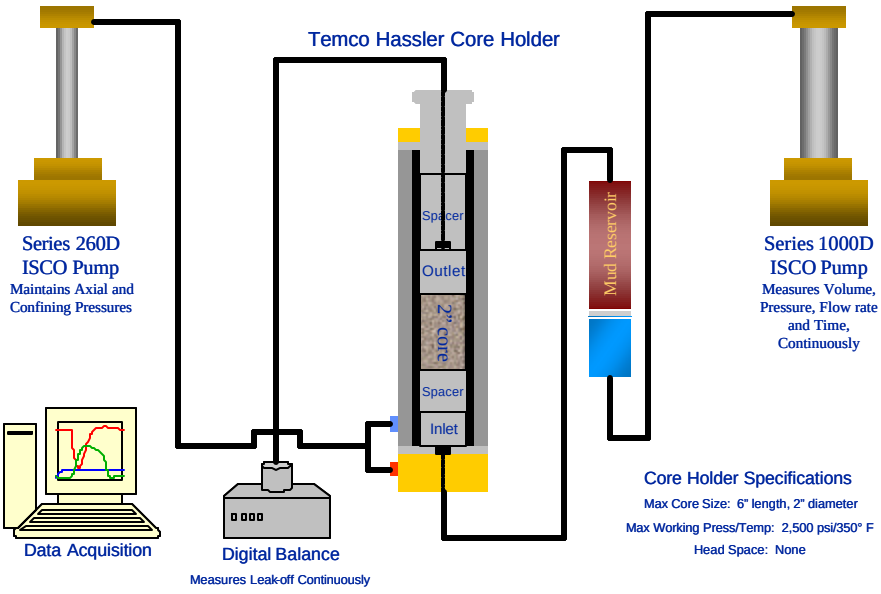

The inlet cap of the coreholder was modified to provide a cone-shaped entry to the fluid, thereby minimizing channeling and problems arising from formation of a non-uniform filter cake. To prevent channeling of mud between a fresh core and walls of the tester, the core is tightly pre-wrapped in a sleeve of thermal shrinking plastic. The pre-wrapped core is evacuated under water to remove all air and to fill the pores with water, and then it is installed inside the coreholder. Confining (radial) pressure is applied to the cell with an Isco syringe pump, and the volume filled by water in the inlet space between the mud front and the bottom of the core – called the "dead volume" – is measured. Fore pressure is also applied with an Isco syringe pump. Net

Leak-Off volume is calculated by subtracting the "dead volume" from the total volume of filtrate collected throughout the 30-minute test.

In all experiments, the confining pressure is maintained at a pressure 500 psig higher than the fore pressure. To eliminate uncertainty in the amount of water trapped in the upstream tubing of the system at the beginning of experiments, a 1 psi check valve is installed on the back end of the tubing close to the filtrate collector. This check valve kept the system completely filled with liquid during all stages of the experiments. A few tests were run with a back-pressure regulator instead of the check valve.

Another apparatus was constructed for low-pressure visualization of fluid flow in sand packs. This consisted of a 1 in OD x 3 ft length polycarbonate tube attached to a 500-mL accumulator and an Isco syringe pump; no confining or back pressure was applied.

RESULTS AND DISCUSSION

In Situ Visualization

Evaluation of the Acoustic Bubble Spectrometer (ABS) in the HTHP Circulating System was carried out with tests at room temperature. Static ABS measurements of a Transparent APHRON ICS™ system containing ~ 40% v/v air were made at 0 psig, 1000 psig, 2000 psig, 2nd 0 psig, and 2nd 0 psig + 15 minutes. Dynamic ABS readings with the pump running at 0.5 gal/min were also recorded at 2000 psig and at 2nd zero psig + 15 minutes. Digital photos of the aphrons in the sight glass were also collected at each of the above static pressures. An example of the static images taken at 0 psig, 2000 psig and 0 psig + 15 min is shown in Figure 9. Some 500 µm glass beads were also introduced into the mud for reference.

Figure 9. Optical Images of Transparent APHRON ICS™ Mud

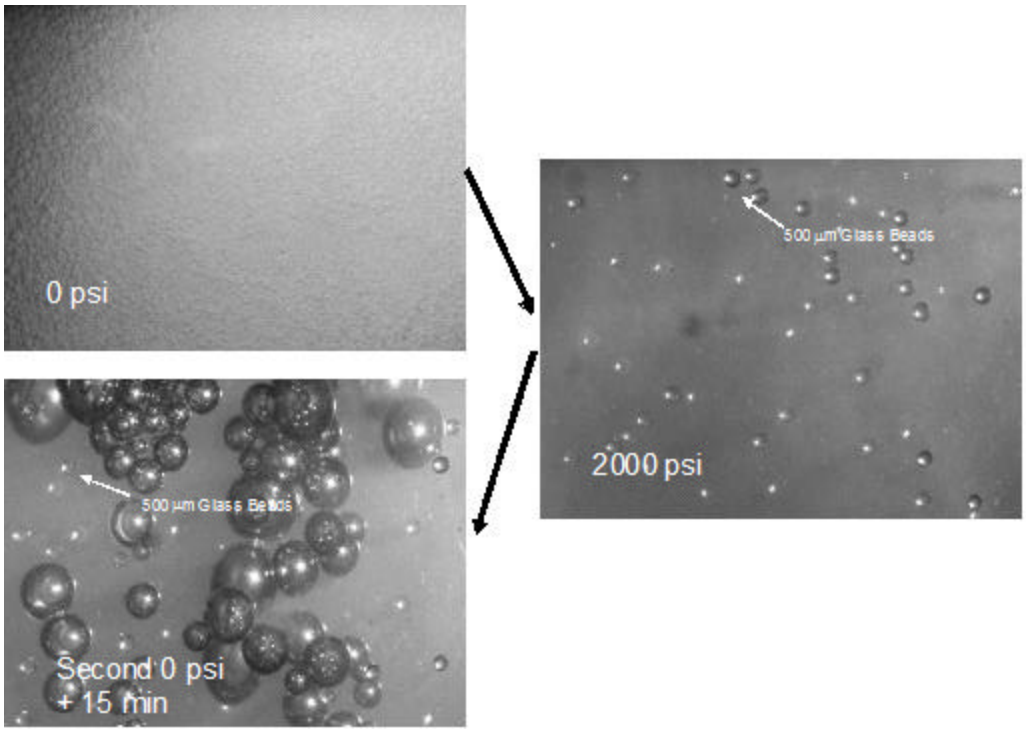

At 0 psig, most of the bubbles are less than 500 µm diameter and appear to average a few hundred µm. After pressurizing to 2000 psig, a few bubbles remain; these appear to be mainly out-

of-focus spheres of a few tens of microns diameter. After the compression/decompression cycle, the bubbles are much larger, though far fewer in number, than they were initially, though they appear to be similar in number to what was observed at 2000 psig. There are a number of other small bubbles that are attached to these larger ones. It is thought that many of the aphrons do not survive compression to 2000 psig, although previous tests have shown that some aphrons – if they are large enough to begin with – can survive to 4000 psig. The air from non-surviving aphrons dissolves in the base fluid, only to be released when the system is depressurized sufficiently to form a supersaturated solution. This air can enter existing aphrons or can form other aphrons that act to feed the larger aphrons.

Under static conditions, the ABS yielded a bubble size distributions (BSD) at 0 psig with average bubble size around 30 µm diameter, compared with an estimated value from optical image analysis of 200 to 300 µm. At 2000 psig, sensitivity of the ABS was too low, and no bubbles were observed. At 2nd 0 psig + 15 min, the ABS showed an average bubble size of about 150 µm, whereas the optical average value was > 1000 µm. Under dynamic conditions, the ABS output was even more problematic. As shown in Figure 10, very similar BSD's were obtained at 2000 psig and at 2nd 0 psig + 15 min.

Figure 10. ABS Output for Dynamic Tests at 2000 and 0 psi

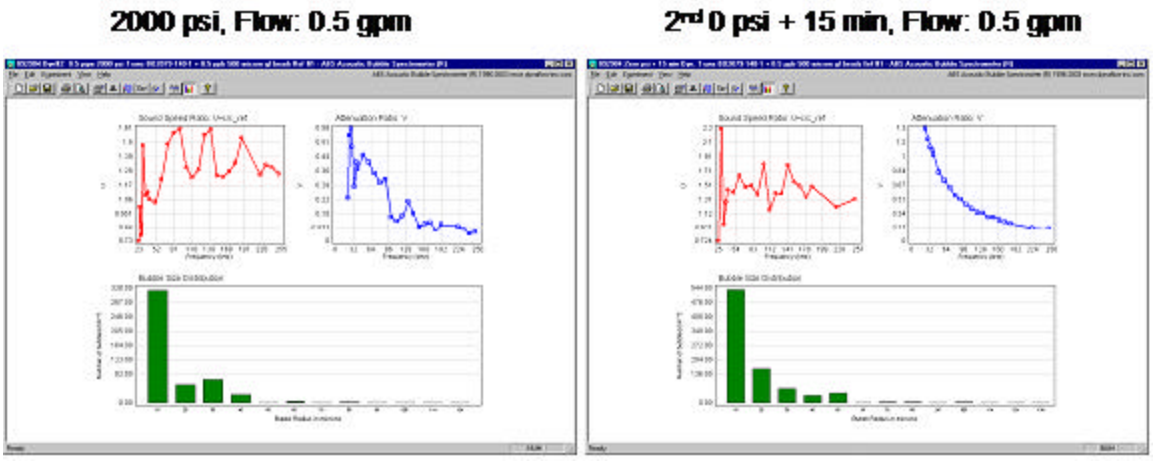

Thus, in agreement with a previous evaluation at ambient conditions, the ABS does not appear to be suitable for monitoring the BSD in APHRON ICS™ drilling fluids. A brief report will be issued next month summarizing these results.

Aphron Air Diffusivity

In addition to examining the effects of pressure on bubble size, a systematic series of tests was begun to determine the effects of pressurization protocol, fluid composition and method of aphron generation on bubble size distribution. It has been hypothesized that slow pressurization or depressurization would be most suitable for maintaining stability of the aphrons, inasmuch as this would allow surfactants in the aphron shell sufficient time to re-organize and maintain an impermeable membrane. Preliminary tests indicated that the rate of pressurization and depressurization has a more complex effect on the stability of the aphrons. In addition, it is also clear that not all of the bubbles are equally stable; indeed, from a few tests it appears that only larger bubbles are able to survive pressurization to a few thousand psi.

More detailed analysis was carried out on the effect of bubble size on aphron survivability. It has been hypothesized that bubble stability increases with decreasing bubble size. While that may be the case for non-interacting bubbles in an isobaric (constant pressure) environment, it does not appear to be the case when aphrons are pressurized. Figure 11 shows the results of pressurization tests carried out on several bubbles. Here initial size measurements of seven well-defined bubbles were determined, as before, at 500 psig. When these are plotted on the graph in the form of Actual (measured) Diameter vs Theoretical (modified Ideal Gas Law) Diameter, they fall on a line with a slope of 1. Pressurizing the system to 1000, 1500 and 2000 psig generated bubbles with the sizes given by the other three points for each bubble. The Theoretical Diameter is given by the expected size obtained using the modified Ideal Gas Law, $P_1V_1/z_1 = P_2V_2/z_2$, where P is the Pressure (1 is for the 500 psig case, 2 is for the other cases), V the volume, and z the compressibility factor for air (obtained from a standard table in the Chemical Engineering Handbook). Figure 11 shows that, under these conditions, the bubbles follow the modified Ideal Gas Law rather closely when their size at 500 psig is above 100 µm diameter, but they deviate markedly when the initial size is 62 µm or less.

Figure 11. Effect of Bubble Size on Bubble Stability

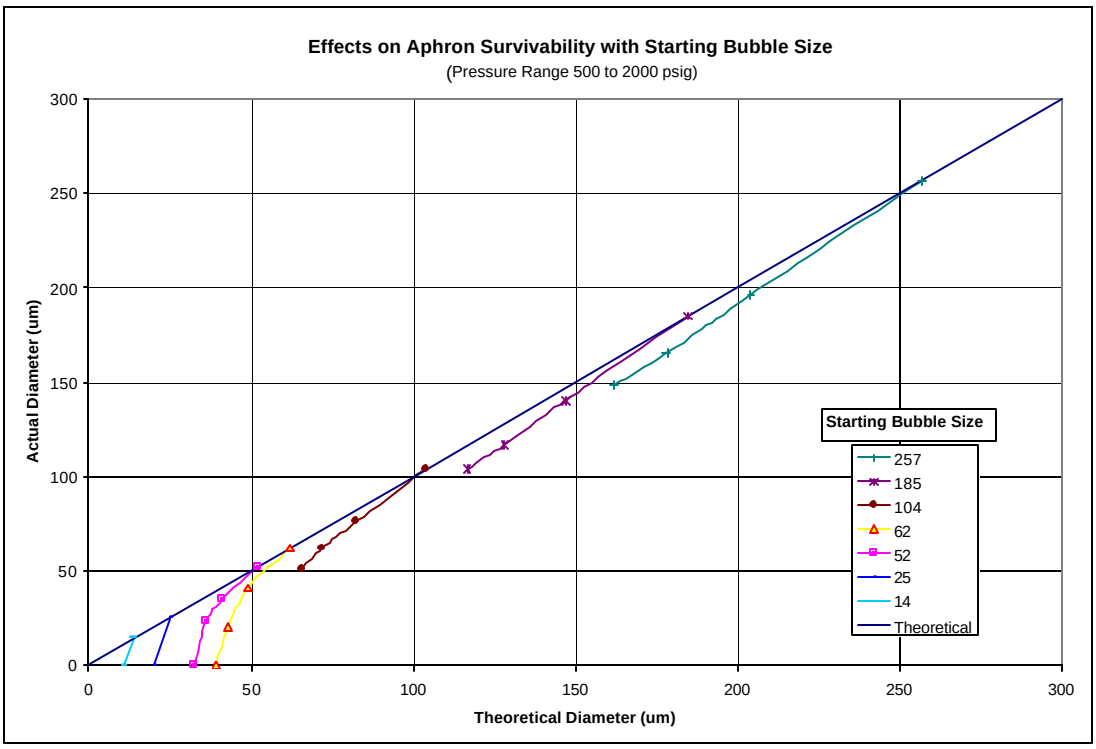

Felix Sebba[5] theorized that an aphron cannot exist below a diameter of 10 to 20 µm. Indeed, it is evident from Figure 11 that there is a critical size below which an aphron cannot exist. When an aphron is squeezed to a size between 25 and 50 µm, at the next pressurization the aphron will shrink to half its size or less. It is in this size range that the aphrons tend to not survive when pressurized above 2000 psig or even above 500 psig. Then again, it should be taken into account that the aphrons could still be there, yet they may be too small to be observed or seen with any software or the human eye.

In addition to pressure, the rate at which pressure is applied appears to have a significant impact on the survivability of aphrons. For example, when an aphron is in an environment where it is being subjected to pressure increases of 500 psig (instead of an immediate pressure increase/decrease), the percentage of original aphrons that are recovered when the system is returned to ambient pressure is greatly reduced. This is contrary to what had been expected,

namely that an aphron would be more stable the slower the pressure ramp. The effect of rate of pressurization on the shrinkage rate of aphrons was examined using two protocols with the Transparent Enhanced APHRON ICS™ drilling fluid:

- Slow Pressurization – 0, 500, 1000, 1500 and 2000 psig, waiting 15 seconds after each new pressure was reached. The system was then depressurized rapidly to 0 psig and pictures were taken at 0, 5, 10, 20 and 30 minutes.

- Fast Pressurization – 0 and 2000 psig, waiting 15 seconds after reaching 2000 psig. The system was then depressurized rapidly to 0 psig and pictures were taken at 0, 5, 10, 20 and 30 minutes.

Figure 12 shows first that aphrons do not recover their initial size very quickly; indeed, it appears that 30 minutes is a minimum amount of time necessary for full recovery. Secondly, aphrons recover at a rate and to a steady state size that depends on the rate of pressurization. In Figure 12, two bubbles of similar size were exposed to the two pressurization protocols described above. The aphron that was pressurized slowly began with an initial diameter of 245 μm but only reached 226 μm 30 min after depressurization, a deficiency of 8%. However, the aphron that was pressurized quickly surpassed its initial size of 200 μm to reach 229 μm, a surplus of 13%. With more time, the aphron that was pressurized slowly might have reached its initial size. The aphron that was pressurized quickly, however, appears to have gained some air. The 13% increase in diameter of that bubble translates to a 44% increase in volume. Indeed, the photographs show that there are fewer small aphrons in the vicinity of this aphron after depressurization than were evident at the beginning of the test. This is consistent with the view that the small aphrons were destroyed during pressurization and the lost air went into solution, only to emerge later when the system was at 0 psig and the system was supersaturated. Some of that air might go to form new aphrons, but it appears that a larger fraction becomes incorporated into existing aphrons. Thus, the aphron shell not only is permeable and susceptible to loss of air, it also appears equally capable of absorbing air from solution.

Figure 12. Effect of Rate of Pressurization Rate on Bubble Size

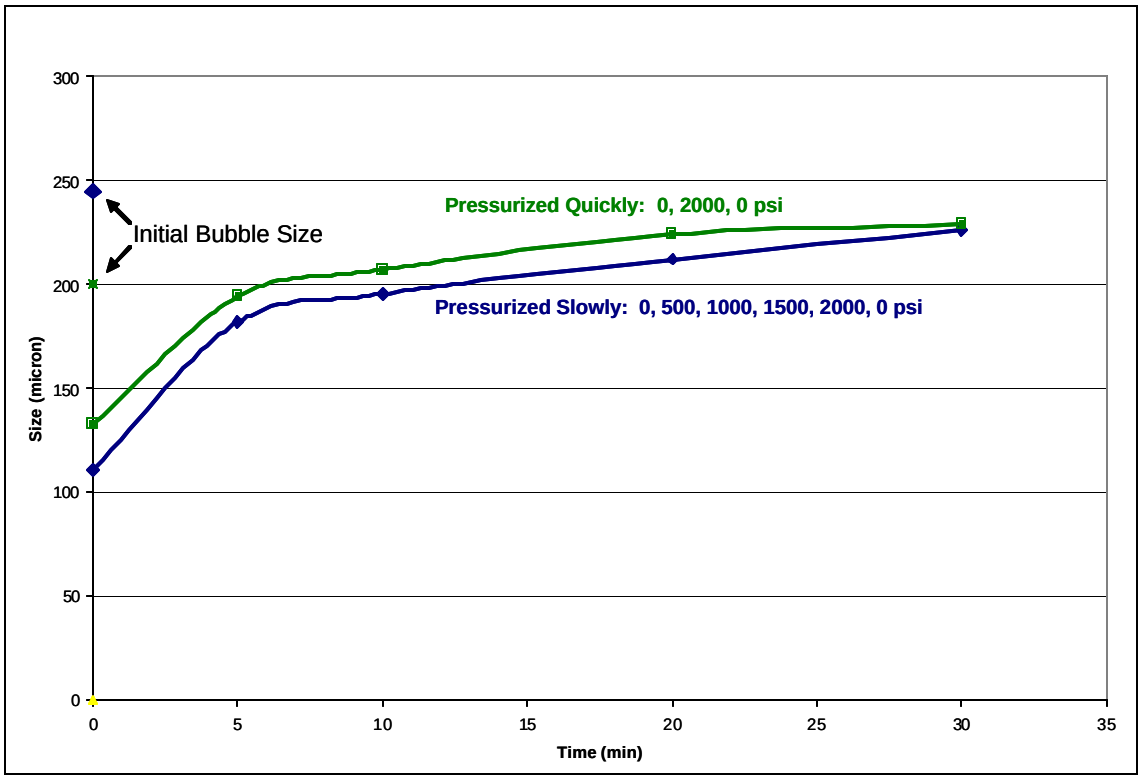

The effect of chemical composition on bubble stability was examined using a Transparent Enhanced (TE) APHRON ICS™ mud and a SuperEnhanced (SE) APHRON ICS™ mud. Figure 13 shows how aphrons from these two muds withstand an applied pressure of 500 psig over a period of time. Initially, the two bubbles used in this comparison were of similar size at 0 psig (355 µm and 388 µm for the TE and SE muds, respectively). Immediately after pressurizing to 500 psig, the two bubbles – according to the Ideal Gas Law – should have been compressed to 109 and 119 µm, respectively. Instead, the bubbles attain sizes of 78 and 101 µm, respectively. It is clear that even immediately after pressurization, the aphron from the TE mud deviates from ideal behavior by almost twice as much (28%) as the aphron from the SE mud (15%). With time, the bubbles from both muds continue to shrink, but the SE aphron shrinks at a much slower rate than the TE aphron. A simple diffusion equation may be applied to approximate the rate of escape of air from the aphron:

$$dS/dt = S_0 \exp(-Dt)$$

where dS/dt represents the change in bubble size (diameter), S_0 is the initial size, and t is time. Rearranging and integrating this expression gives

$$S/S_0 = \exp(-Dt)$$

For the SE mud, S_0 = 101 µm, and S = 75 µm at 39 min. This gives D = 0.0076 min^{-1}. For the TE mud, the only measurement we have besides S_0 = 78 µm is S = 52 µm at 5 min, which gives D = 0.081 min^{-1}. Thus, the rate of loss of air is almost an order of magnitude greater in aphrons from the TE mud than from the SE mud. This conclusion is probably conservative, as it appears from Figure 3 that the rate of air loss accelerates after 5 min.

It should be noted that the exponential expression above does not fit either set of data particularly well. One possibility is competition of another mechanism. In light of previous data which suggested that there is a minimum size below which aphrons cannot exist, aphrons below or near such a threshold size may degrade structurally. This hypothetical bimodal mechanism – diffusion and structural degradation – will be looked at more closely during Phase II of this project.

Figure 13. Effect of Fluid Composition on Aphron Stablity

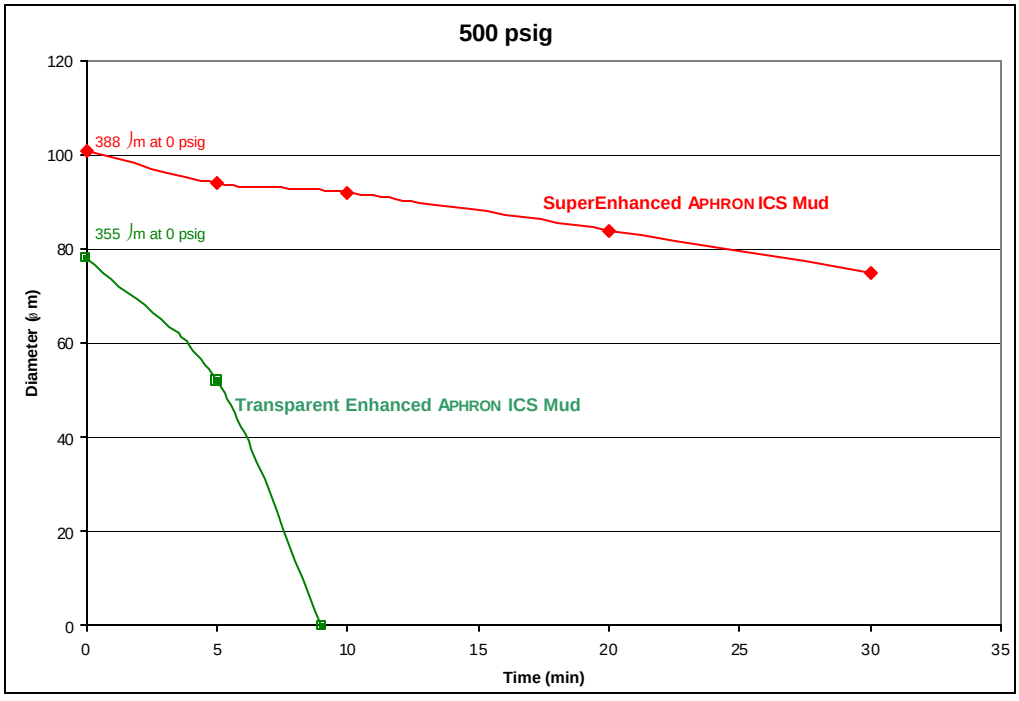

A topical report will be issued next month covering this work on diffusivity of air from aphrons.

Aphron Hydrophobicity

A modification of the apparatus shown in Figure 6 employs two glass syringes connected with a disposable filter of pore size much smaller than the average bubble size. However, very little force is required to squeeze over-size bubbles through the filter; indeed, repeated flow back and forth was found to simply "polish" the bubbles to produce a relatively narrow bubble size distribution of ever decreasing average bubble size. Not only did the bubbles go through the pores with no problem, they also did not appear to stick to anything, including each other. Indeed, the notable absence of aphrons on the glass walls of the syringes suggested that other mineral surfaces be tried. In a previous study, APHRON ICS™ muds were spread on Berea sandstone and Aloxite cores. When the cores were swirled in deaerated mud, none of the aphrons were found to be visibly attached to the mineral surfaces.

To get a better idea of the surface character of the aphrons, an alternative technique was devised to better evaluate the tendency for aphrons to aggregate. The idea was to get two or more bubbles to collide and observe whether they stuck together. If they moved as an aggregate, it meant that the bubbles had some affinity for each other. If they traveled on different paths, that meant that the bubbles did not stick together and, therefore, had little affinity for each other. Several techniques were tried, but the most promising (see Figure 14) involved a glass vessel through which the Transparent Enhanced (TE) APHRON ICS™ mud moved vertically and the bubbles were injected through two open tubes capped with septa and positioned opposite each other at angles of 45 degrees to the vertical.

It was learned that injection of air through a single syringe resulted in a string of bubbles that would flow as an aggregate. However, the fluid traveled in plug flow and did not give the bubbles an opportunity to separate. So, another method was developed to investigate how the bubbles act when some mechanical force is applied on them. For this, some centrifuged TE APHRON ICS™ Mud was spread as a thin layer (a smear) on a standard microscope slide.

Figure 14. Air Injection Test Set-Up

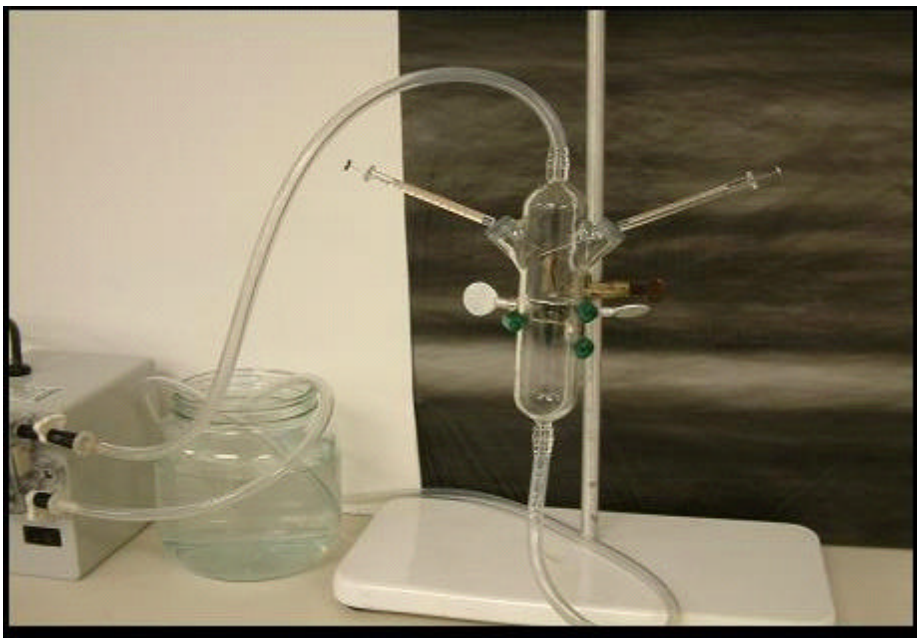

The set-up for this is shown in Figure 15. A string of aphrons was created, as above, by injection of air through a syringe. Then the fluid around the aphrons was moved around by swirling it using the syringe needle. It was clear from this simple procedure that the bubbles did not stay together. An example of this is shown in Figures 16 and 17.

Figure 15. Set-Up for Microscope Slide Smear Test

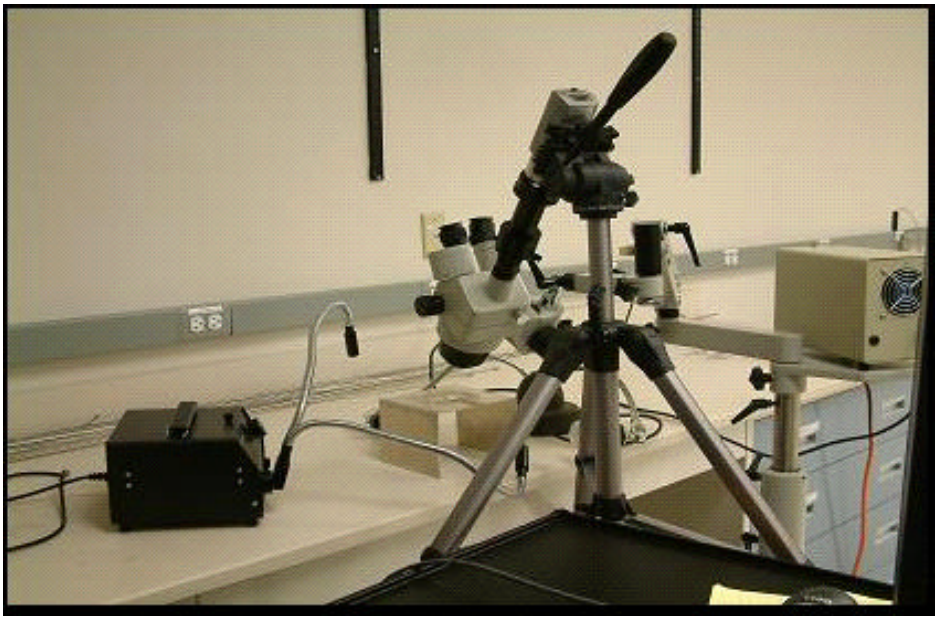

Figure 16. An Aggregate of Aphrons Formed during Bubble Creation

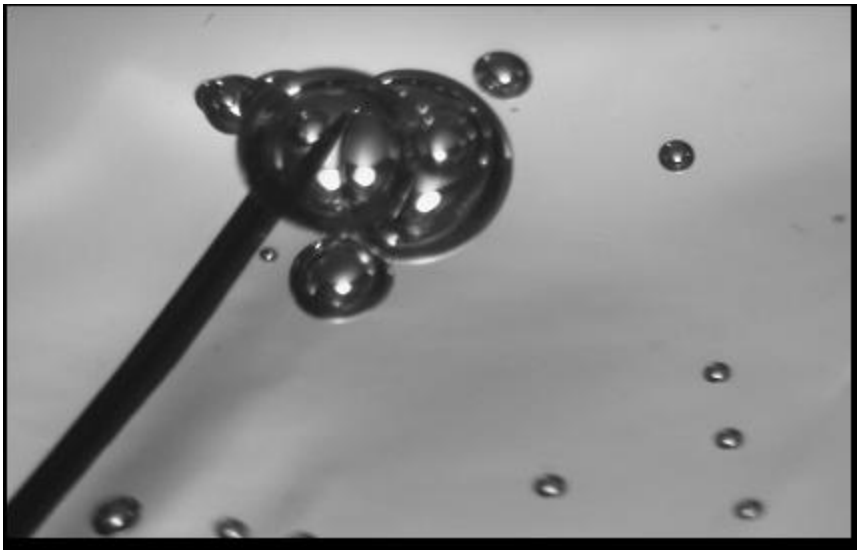

Figure 17. The Aphron Aggregate Breaks Up When Mild Swirling Force Is Applied

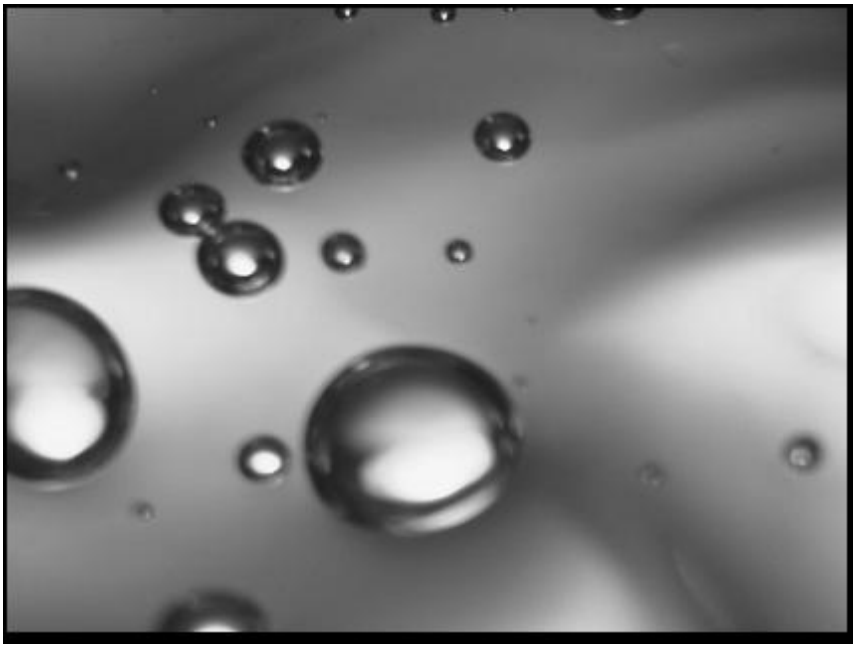

Repeated tests showed the same result. Thus, it appears that aphrons have little or no affinity for each other, nor for silica or alumina surfaces. A topical report of these results will be issued next month.

Sealing of Permeable and Fractured Media

Leak-Off Tests

The tests were conducted with FAO-5 (nominal air permeability 5 darcy) Aloxite cores 1-1/2" diameter x 2" length, using 500 psig and 1000 psig fore pressure. Super Enhanced APHRON ICS™ mud was used in all cases, and the effect of aphrons on leak-off was determined with back-to-back tests with samples containing air and samples that had been deaerated by centrifugation.

All tests resulted in plugging of the cores and collection of clear filtrate. Figure 18 shows the results obtained at the two fore pressures comparing deaerated mud with mud containing 21% air. As Figure 18 reveals, Leak-Off increased with increasing fore pressure and no air. These effects appear to be associated solely with the spurt loss at the beginning of the run.

Figure 18. Leak-Off Tests with 5-Darcy Aloxite Cores at Various Inlet Pressures

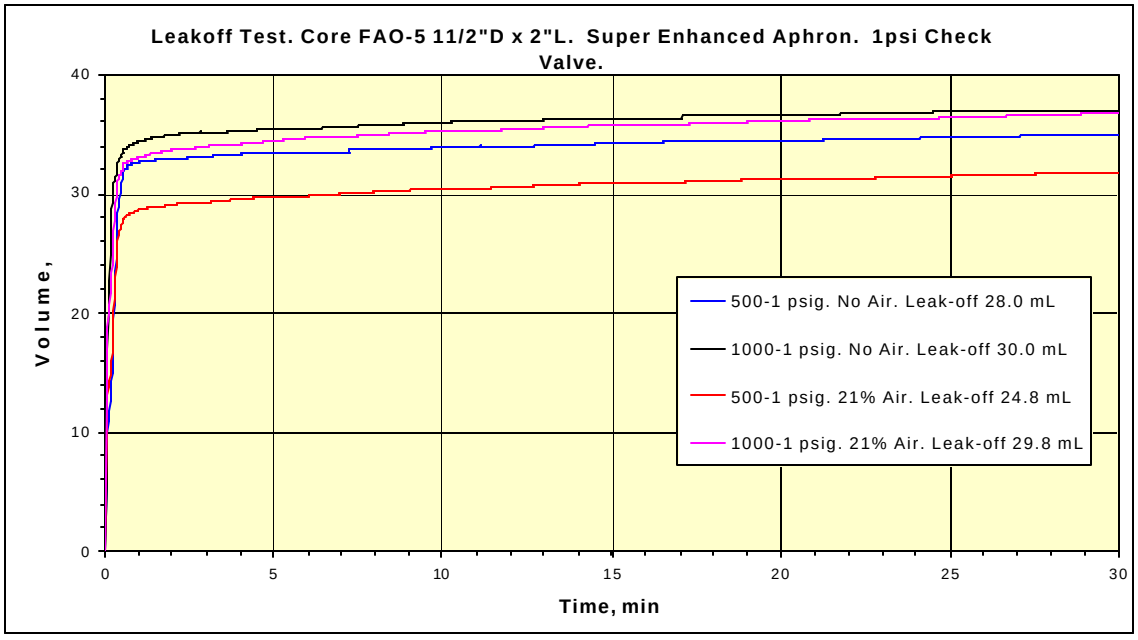

To determine the effect of core permeability on Leak-Off, tests were conducted at 500 psig fore pressure with Aloxite cores WFAO-A (nominal air permeability 0.75 darcy) and FAO-10 (nominal air permeability 10 darcy) 1-1/2" diameter x 2" length. The results are compared with those using FAO-5 in Figure 19.

Figure 19. Effect of Aloxite Core Permeability on Leak-Off at 500 psig Fore Pressure

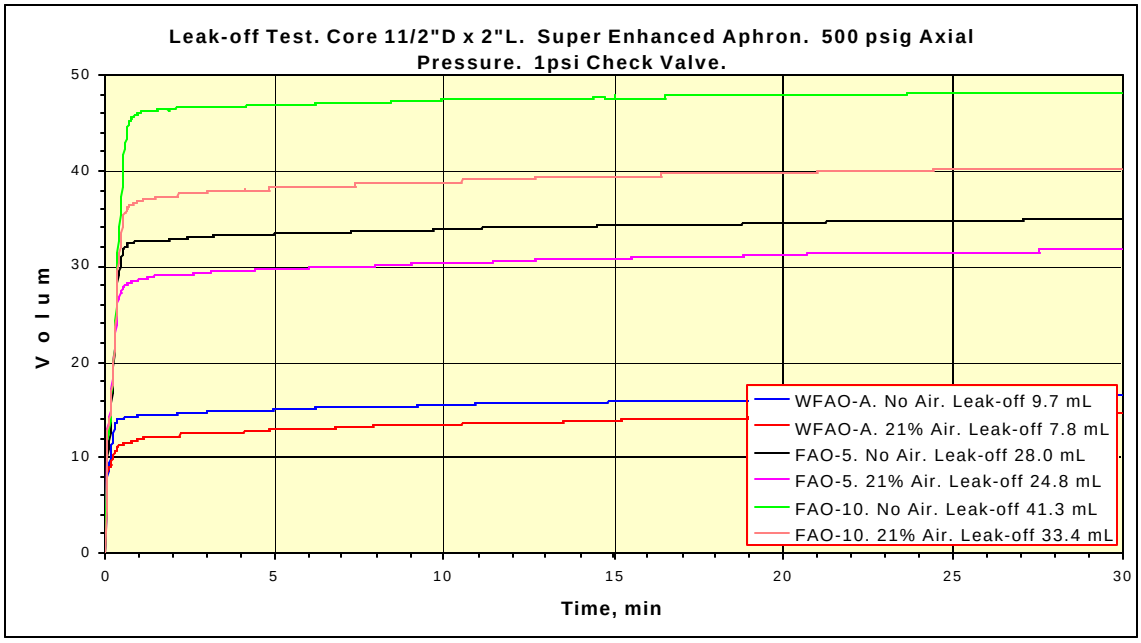

It is clear that Leak-Off increases with increasing permeability of the core, and again it is the spurt loss which is primarily affected. It is also clear that the muds containing air gave consistently lower Leak-Off than the deaerated samples, and the differential in Leak-Off appears to increase with increasing core permeability. This differential between deaerated mud and mud containing 21% was 2.1 mL, 3.2 mL and 7.9 mL for WFAO-A, FAO-5 and FAO-10 cores, respectively.

Finally, the effect of core length on Leak-Off was determined using two FAO-10 cores in series, which resulted in an effective core length of 4" instead of the standard length of 2". The result of this experiment is show on Figure 20.

Figure 20. Leak-Off Tests with Two 10-Darcy Aloxite Cores of 4" Total Length

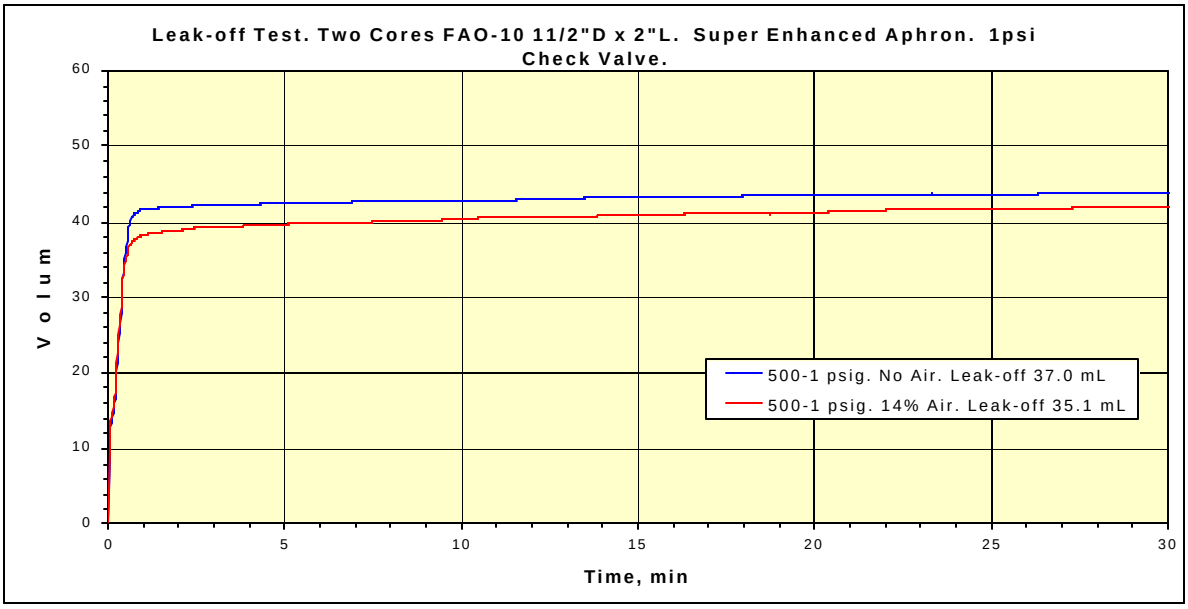

Leak-Off for the deaerated mud in the 4" core was a few mL less than that observed for the 2" core (see Fig. 19), and, although the Leak-Off when air (14% v/v) was introduced into the sample was a little lower than for the deaerated mud, it is probably within experimental error. Other than normal scatter, it is speculated that the effect of air on Leak-Off may be non-linear, i.e. 21% air (see Fig. 19 again) may have a significantly larger affect on Leak-Off than expected from the simple ratio of air volumes.

Flow Visualization

An unusual phenomenon was observed for flow of the SuperEnhanced APHRON ICS™ mud in the transparent pipe. The bubbles appeared to move faster than the bulk fluid and to concentrate at the front of the moving mud. This was initially thought to be related to a "jump" effect that viscoelastic fluids are known to impart to bubbles. Another phenomenon sometimes seen in two phase flow with a low-density internal phase, namely congregation of the bubbles near the pipe wall, was not observed. The anomalous behavior of the bubbles was observed with both 20/40 and 70/100 sand packs, as long as there was a pressure difference along the length of the sand pack. The most pronounced effect was observed with the 20/40 mesh sand pack filled with wa-

ter. Unfortunately, the brown color of both the sand and the APHRON ICS™ mud made for difficult viewing of this phenomenon.

To overcome these hurdles a new system was constructed using a clear acrylic pipe, and a Transparent Enhanced APHRON ICS™ fluid sample was substituted for the SuperEnhanced mud sample. From previous experience, aphrons are lighter in color than the base fluid, and the contrast is highest with small bubbles and a strong color for the base fluid. To record the phase behavior of the mud during flow, the transparent mud was saturated with RIT #6 blue dye. The front end of the acrylic pipe was connected to a valve and to an accumulator with a piston. The back end of the pipe was opened to the atmosphere. At the beginning of the experiment, the valve was closed and a pressure of 100 psig was applied to the mud in the accumulator. Then the valve was opened, and mud began to move through the sand pack.

Figure 21 shows one exposure from the video stream of the test. The colored mud is moving from right to left, and the leading edge of the fluid has passed the middle of the pipe. At the leading edge, the fluid is much lighter in color, and microscopic examination reveals that region to be composed primarily of bubbles. The highest color intensity is at the entrance, and few bubbles are apparent. One may argue that the loss of color while traversing the sand pack was due to depletion of the dye, but it was evident both from examination during and after the test, that little or no dye had adsorbed onto the sand grains.

Figure 21. Dyed Transparent APHRON ICS™ Mud Flowing through 20/40 Sand Pack

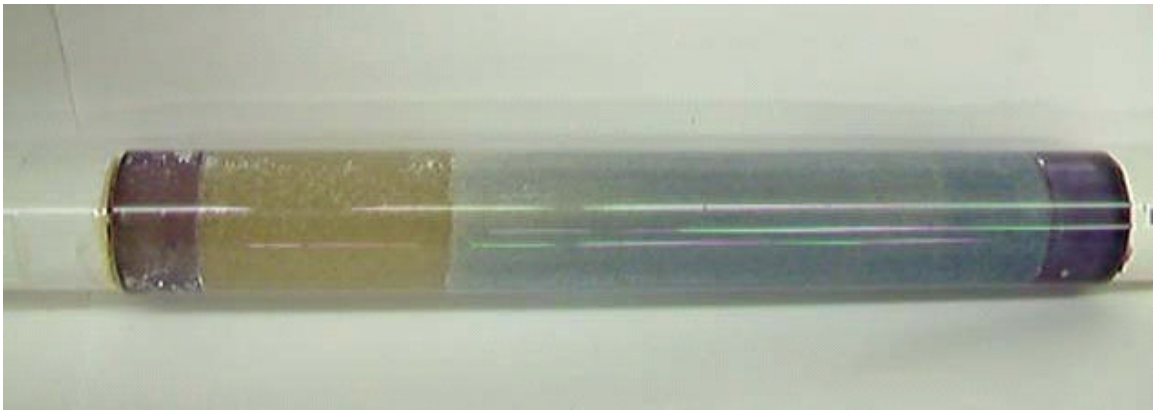

Feedback from researchers at Texas A&M University on this phenomenon indicates that our observations are consistent with those expected for a dispersed low-density internal phase. The Navier Stokes expression for settling of a dense particle through a liquid applies equally well for creaming or buoyancy of a light "particle." This movement is, of course, driven by the force of gravity. However, when the force is a pressure differential, which is defined as force/area, the effect is similar, and transport of the internal phase will be in the direction of the pressure drop. The greater the pressure drop, density difference and bubble size, the greater will be the relative velocity of a bubble. This will be examined in much greater detail during Phase II.

CONCLUSIONS

Tests carried out at pressures up to 2000 psig, with and without flow, confirm a previous finding at ambient conditions that Acoustic Bubble Spectroscopy (ABS) does not produce a sufficiently accurate measurement of bubble size distribution (BSD) in aphron drilling fluids. Instead, direct optical imaging is recommended to determine the effects of environmental variables on bubble size. The development of an ultra-shallow high-pressure viewing cell enables imaging of opaque fluids and obviates the need for ABS in this project.

Imaging of aphron drilling fluids at elevated pressures showed that aphrons can survive compression to at least 4000 psig. However, the number of visible aphrons at that pressure is small, and even the survivors have a limited life. Compression of large aphrons initially results in volume reduction that is inversely proportional to the absolute pressure. Over time, they shrink further at a rate that depends on fluid composition, bubble size, and rate of pressurization and depressurization. When the bubbles reach a critical minimum size -- on the order of 50 µm diameter -- they undergo a structural change that leads to their collapse, and the aphrons vanish.

Leak-Off tests at fore pressures as high as 1000 psig demonstrated that the base fluid is primarily responsible for sealing permeable zones and is capable of sealing rock as permeable as 80 darcies. However, properly designed aphrons can reduce these losses even further. Although the amount of air in a typical aphron drilling fluid is less than 0.02% w/w, aphrons can affect the invasion rate of the fluid because of "bubbly flow." Under the influence of a pressure differential, aphrons move at a velocity much greater than the liquid phase. Thus, they can accumulate at the fluid front and inhibit movement of the liquid. At the same time, aphrons have very little affinity for each other or for the mineral surfaces in rock formations encountered during drilling; thus, aphrons resist agglomeration and coalescence and can be pushed back out easily by reversing the pressure differential.

REFERENCES

1. Montilva, J., Ivan, C.D., Friedheim, J. and Bayter, R.: "Aphron Drilling Fluid: Field Lessons From Successful Application in Drilling Depleted Reservoirs in Lake Maracaibo," OTC 14278, presented at the 2002 Offshore Technology Conference, Houston, May 6-9, 2002.
2. Growcock, F.B., Simon, G.A., Rea, A.B., Leonard, R.S., Noello, E. and Castellan, R.: "Alternative Aphron-Based Drilling Fluid," IADC/SPE 87134, presented at the 2004 IADC/SPE Drilling Conference, Dallas, Mar. 2-4, 2004.
3. Brookey, T., Rea, A. and Roe, T.: "UBD and Beyond: Aphron Drilling Fluids for Depleted Zones," presented at IADC World Drilling Conference, Vienna, Austria, Jun. 25-26, 2003.
4. Growcock, F.B., Simon, G.A., Guzman, J., and Paiuk, B.: "Applications of Novel Aphron Drilling Fluids," AADE-04-DF-HO-18, presented at the AADE 2004 Drilling Fluids Conference, Houston, TX, Apr. 6-7, 2004.
5. Sebba, F.: Foams and Biliquid Foams – Aphrons, John Wiley & Sons Ltd, Chichester (1987).
6. White, C.C., Chesters, A.P., Ivan, C.D., Maikranz, S. and Nouris, R.: "Aphron-Based Drilling Fluid: Novel Technology for Drilling Depleted Formations," World Oil, vol. 224, no. 10 (Oct. 2003).

LIST OF ACRONYMS AND ABBREVIATIONS

ABS = Acoustic Bubble Spectroscopy

APHRON ICS™ = Aphron Invasion Control System

BSD = Bubble Size Distribution

DO = Dissolved Oxygen

EMI- = Experimental M-I *LLC* product

FloVis Plus = Xanthan Gum polymer

gpm = gallons per minute

HTHP = High Temperature and High Pressure

OD = Outer Diameter

psig = Gauge pressure in psi

SE = SuperEnhanced